Second-order self-force for eccentric EMRIs in Schwarzschild spacetime

Wei Yi-Xiang, SCUT

2025/10/19

Based On

Wei YX, Zhu XL, Zhang JD, Mei JW. PRD, 2025, 112(6): 064048.

I. Background

II. Methods

III. Main Results

IV. Conclusion

The Extreme Mass Ratio Inspirals

The Extreme Mass Ratio Inspirals:

- Supermassive black hole with mass $M = 10^5 \sim 10^7 M_\odot$
- Steller-mass compact object with mass $m = 10^0 \sim 10^2 M_\odot$.

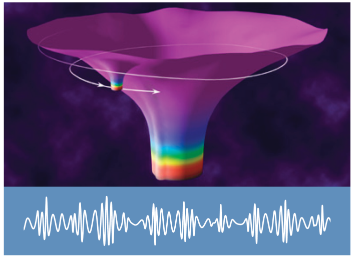

The mass ratio $\varepsilon = m/M = 10^{-5} \sim 10^{-7}$.

A key detection target of space-based detectors such as LISA, TianQin and Taiji.

EMRI signals are rich in information, including the shape of SBH[1], the environment near SBH[2],such as dark matter halo[3].

1. Zi T, Zhang J, Fan H M, et al. PRD, 2021, 104(6): 064008.
2. Wang Y, Han W, Wu X, et al. CQG, 2025, 42(17): 175007.
3. Zhang C, Fu G, Dai N. JCAP, 2024, 2024(04): 088.

Accuracy Requirements

The `Matched Filter` method is needed for identify the EMRI signal.

An error at $\sim 1\,\mathrm{rad}$ or half circle for the entire observation is unacceptable.

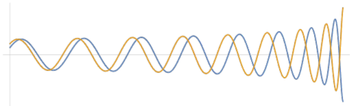

The acceleration errors will accumulate throughout the entire inspiral phase, ultimately reaching ε^{-2} level for phase error:

$$
\begin{aligned}
a &\sim \mathrm{d}^2\Phi/\mathrm{d}t^2 \\
\Delta a &\sim \Delta\Phi/T_{\mathrm{total}}^2 \sim \varepsilon^2 \Delta\Phi
\end{aligned}
$$

The calculation of acceleration must be exact at ε^2 order at each circle!

The Self-Force Method

A precise calculation of real space-time $\tilde{g}_{\mu\nu}$ evolution is too expensive in practice.

$$\begin{cases} \tilde{R}_{\mu\nu} - \frac{1}{2}\tilde{g}_{\mu\nu} = 8\pi T_{\mu\nu} \\ u_\mu \tilde{\nabla}_\nu u^\nu = 0 \end{cases}$$

To simplify the mission, we treat the SBH metric as the back-ground metric:

$$\begin{cases} \tilde{g}_{\mu\nu} = g^{(0)}_{\mu\nu} + \varepsilon h^{(1)}_{\mu\nu} + \varepsilon^2 h^{(2)}_{\mu\nu} + \cdots \\ u_\mu \nabla^{(0)}_\nu u^\nu = \varepsilon f^{(1)}_\mu + \varepsilon^2 f^{\nu\,(2)} + \cdots \end{cases}$$

Where the f_μ term originates from the self-gravitational field of the small body and drives its deviation from the background geodesic, hence referred as **the self-force**.

Current State of Research

Background	Schwarzschild		Kerr	
trajectory	quasi-circular	generic	equatorial	generic
1st SF	Warburton, et al. 2012.	Van De Meent, et al. 2018	Lynch, et al. 2022	Lynch, et al. 2024
2nd SF	Warburton, et al. 2023	On-Going	NONE	

[1] Warburton N, Akcay S, Barack L, et al. PRD, 2012, 85(6): 061501. arXiv:1111.6908.

[2] Van De Meent M, Warburton N. CQG, 2018, 35(14): 144003. arXiv:1802.05281.

[3] Lynch P, van de Meent M, Warburton N. CQG, 2022, 39(14): 145004. arXiv:2112.12265.

[4] Lynch P, Witzany V, van de Meent M, et al.CQG, 2024, 41(22): 225002. arXiv:2405.21072.

[5] Wardell B, Pound A, Warburton N, et al. PRL, 2023, 130(24): 241402. arXiv:2112.12265.

Overview

Process Flow

$$u^\mu \nabla_\mu u^\nu = f^\nu$$

Coordinates to parameters

$$\frac{\mathrm{d}I_a}{\mathrm{d}t} = \varepsilon f_a^{(1)} + \varepsilon^2 f_a^{(2)} + \mathcal{O}(\varepsilon^3)$$

$$I_a = (p, e)$$

$$G^{(1)}_{\mu\nu}[h^{(2)}] = 8\pi T^{(2)}_{\mu\nu}[I^A, h^{(1)}] - G^{(2)}_{\mu\nu}[h^{(1)}, h^{(1)}]$$

$$f_a^{(n)}(h_{\mu\nu}) = f_a^{(n)}(h^R_{\mu\nu})$$

Self-force calculation

$$h^{(n)}_{\mu\nu} = h^{\mathcal{P}(n)}_{\mu\nu} + h^{\mathcal{R}(n)}_{\mu\nu}$$

$$\tilde{t} = \varepsilon t$$

Separation of Oscillation & Dissipation

$$\frac{\mathrm{d}I^{(0)}}{\mathrm{d}\tilde{t}} = F_0[I^{(0)}(\tilde{t}), h^{(1)}_{\mathcal{P}}(\tilde{t}), (\tilde{t})]$$

$$\frac{\mathrm{d}I^{(1)}}{\mathrm{d}\tilde{t}} = F_1[I^{(0)}(\tilde{t}), I^{(1)}(\tilde{t}), h^{(1)}_{\mathcal{R}}(\tilde{t}), h^{(2)}_{\mathcal{R}}(\tilde{t}), (\tilde{t})]$$

Programming

Osculating Geodesic Method

The parameters of trajectory evolves slowly.

Real evolution of the secondary can be treated as the evolution of geodesics in background spacetime.

For Schwarzschild spacetime, A generic bounded geodesic can be described by $I_a = (p, e)$ 。

$$r = \frac{pM}{1 + e\cos(\chi - \chi_0)}$$

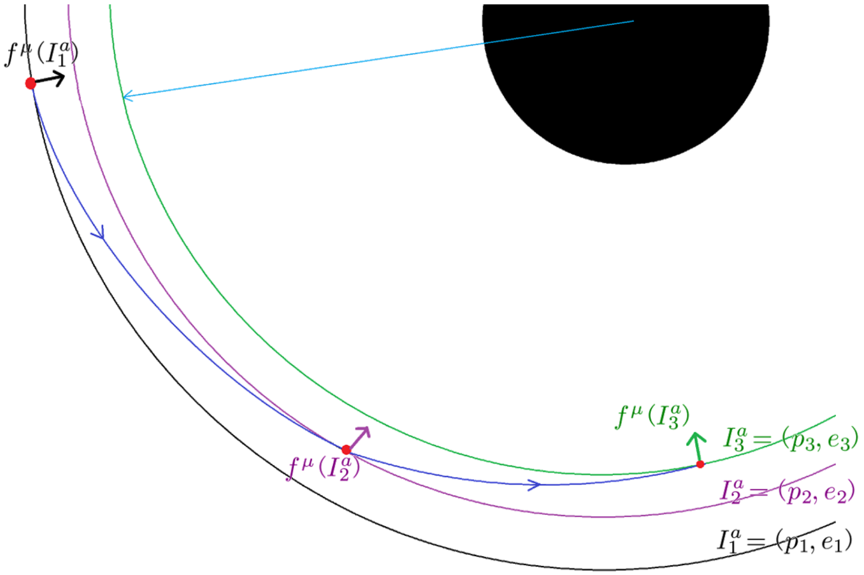

Coordinates to Parameters

Osculating Geodesic Method

The parameters of trajectory evolves slowly.

Real evolution of the secondary can be treated as the evolution of geodesics in background spacetime.

The time-domain evolution of self-force in real trajectory can replaced by the frequency-domain evolution of SF in a background geodesic.

$$\frac{\mathrm{d}I_a}{\mathrm{d}\chi} = c_a^{(r)}[I_b,\chi]\,f_r + c_a^{(\varphi)}[I_b,\chi]\,f_\varphi$$

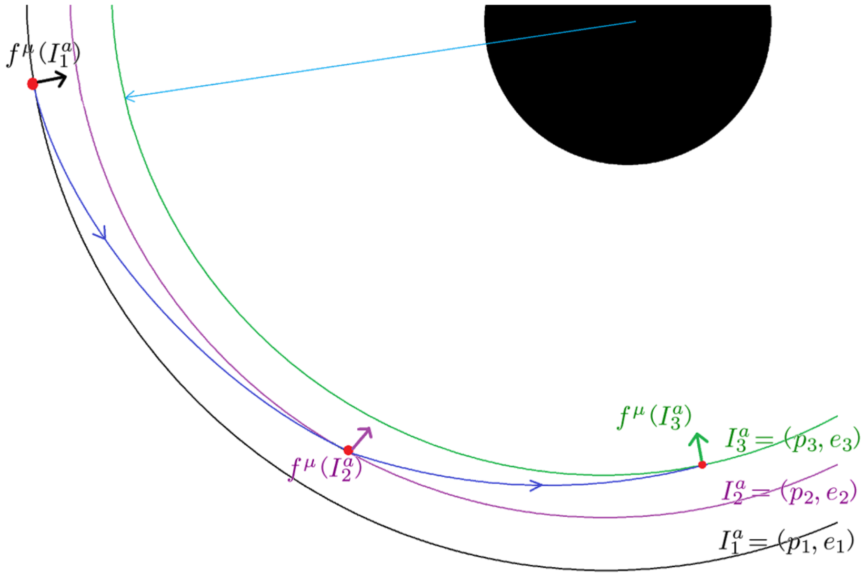

Self-Force from Field

The self-gravitational field of SCO can be divided as $h_{\mu\nu}=h^S_{\mu\nu}+h^R_{\mu\nu}$

- The singular part $h^S_{\mu\nu}$ is the unphysical self-energy part;
- Only regular part $h^R_{\mu\nu}$ contribute to the self-force[4]:

$$
\begin{aligned}
f^\mu \;=\; & -\frac{1}{2}\varepsilon\left(g^{\mu\alpha}+u^\mu u^\alpha\right)\left(2\nabla_\gamma h^{R(1)}_{\sigma\beta}-\nabla_\sigma h^{R(1)}_{\gamma\beta}\right)u^\beta u^\gamma \\
& +\frac{1}{2}\varepsilon^2\left(g^{\mu\alpha}+u^\mu u^\alpha\right)u^\beta u^\gamma\left[h^{R(1)\sigma}_{\gamma\alpha}\left(2\nabla_\gamma h^{R(1)}_{\sigma\beta}-\nabla_\sigma h^{R(1)}_{\gamma\beta}\right)-\left(2\nabla_\gamma h^{R(2)}_{\sigma\beta}-\nabla_\sigma h^{R(2)}_{\gamma\beta}\right)\right] \\
& +\mathcal{O}\left(\varepsilon^3\right)
\end{aligned}
$$

---

4. POUND A. Second-order gravitational self-force[J]. PRL2012, 109(5): 051101.

Puncture Fields

There is no exact form of $h^{S}_{\mu\nu}$, to subtract the divergence in numerical computation, we use a puncture field $h^{\mathcal{P}}_{\mu\nu}$ with analytical form to replace $h^{S}_{\mu\nu}$, while ensuring the invariance of the self-force:

$$\begin{aligned} \lim_{x\to\gamma}(\bar{h}^{S}_{\mu\nu}-\bar{h}^{\mathcal{P}}_{\mu\nu}) &= 0 \\ \lim_{x\to\gamma}\nabla_{\alpha}(\bar{h}^{S}_{\mu\nu}-\bar{h}^{\mathcal{P}}_{\mu\nu}) &= 0 \end{aligned}$$

By cutoff the expansion of trace-reversed $\bar{h}^{S}_{\mu\nu}$ at certain order, we have a puncture field $\bar{h}^{\mathcal{P}}_{\mu\nu}$

$$\bar{h}^{\mathcal{P}}_{\mu\nu} = 4m\, g_{\mu}{}^{\bar{\alpha}} g_{\nu}{}^{\bar{\beta}}\left[\frac{u_{\bar{\alpha}}u_{\bar{\beta}}}{\bar{s}}+\mathcal{O}(\lambda)\right]$$

where $\bar{s}^2=(g_{\bar{\alpha}\bar{\beta}}+u_{\bar{\alpha}}u_{\bar{\beta}})\,\sigma^{\bar{\alpha}}\sigma^{\bar{\beta}}$,and $\sigma^{\bar{\alpha}}$ is the derivative of Synge function.

- higher order formula will give a higher convergence speed.

we calculate the puncture fields to the sub-leading order by the xAct.[5]

$$\bar{h}^{\mathcal{P}}_{\alpha\beta} = \frac{m}{\lambda}\frac{A_{\alpha\beta}}{\rho}+m\left[\frac{B^{i}_{\alpha\beta}\Delta x_i}{\rho}+\frac{C^{ijk}_{\alpha\beta}\Delta x_i\Delta x_j\Delta x_j}{\rho^3}\right]+\mathcal{O}(\lambda)$$

$$A_{00}=\frac{4(r-2M)^2}{r^2}(u^t)^2,\quad A_{01}=-4u^tu^r,\quad A_{03}=-4r(r-2M)u^tu^\phi,\quad A_{11}=\frac{4r^2}{(r-2M)^2}(u^r)^2,$$

$$A_{13}=\frac{4r^3}{r-2M}u^ru^\phi,\quad A_{33}=4r^4(u^\phi)^2,\quad B^r_{00}=\frac{2M(r-2M)}{r^3}(u^t)^2,\quad B^r_{01}=\frac{6M}{r(r-2M)}u^tu^r,$$

$$\ldots\ldots$$

5. Wei YX, Zhu XL, et al. PRD, 2025, 112(6): 064048.

Two-Timescale Expansion

For a dissipative oscillation system, We have two different timescales corresponding to two different physical origins.

- The short/fast timescale τ for the oscillation period;
- The long/slow timescale $\tilde{t}=\varepsilon t$ for the characteristic time of dissipation.

By expanding functions of t to functions of $(\tau,\tilde{t})$,

$$y(t) \sim G(\tilde{t}) \sum_n \varepsilon^n F_n(\tau)$$

We can decouple two distinct physical processes, significantly speed up the calculation by transforming the oscillatory component into the frequency domain.

Overview

Two-Timescale Expansion for Generic Schwarzschild EMRIs

For a generic bounded geodesic in Schwarzschild spacetime, we have

- Slow variables: two angular velocities Ω_φ, Ω_r;
- Fast variables: two action-angles $q_r = \Omega_r t, q_\phi = \Omega_\phi t$.

The equations of motion can be expanded into

$$\frac{\mathrm{d}q_r}{\mathrm{d}t} = \Omega_r[I_c(\tilde{t})] + \sum_{n=1}^{+\infty} \varepsilon^n g_r^{(n)}(q_r, I_c, \tilde{t}) \quad , \quad \frac{\mathrm{d}\Psi}{\mathrm{d}t} = \Omega_r[I_c(\tilde{t})],$$

$$\frac{\mathrm{d}I_a}{\mathrm{d}t} = \sum_{n=1}^{+\infty} \varepsilon^n G_r^{(n)}(q_r, I_c, \tilde{t}) \quad , \quad \frac{\mathrm{d}q_\phi}{\mathrm{d}t} = \Omega_\phi[I_c(\tilde{t})]$$

We have introduced a new slow variable Ψ to simplify equations.

Expanding the EoM order by order,we have

$$
\begin{aligned}
\Omega^{(0)}(\tilde{t})\partial_\Psi I_a^{(0)} &= 0 \\
\Omega^{(0)}(\tilde{t})\partial_\Psi q_r^{(0)} &= \Omega_r\left(I_c^{(0)}\right) \\
\Omega^{(0)}(\tilde{t})\partial_\Psi I_a^{(1)} &= G_a^{(1)}\left(q_r^{(0)}, I_c^{(0)}, \tilde{t}\right) - \Omega^{(1)}(\tilde{t})\partial_\Psi I_a^{(0)} - \partial_{\tilde{t}} I_a^{(0)} \\
\Omega^{(1)}(\tilde{t})\partial_\Psi q_r^{(0)} &= I_b^{(1)}\partial_{I_b}\Omega_r\left(I_c^{(0)}\right) + g_r^{(1)}\left(q_r^{(0)}, I_c^{(0)}, \tilde{t}\right) \\
&\quad -\Omega^{(0)}(\tilde{t})\partial_\Psi q_r^{(1)} - \partial_{\tilde{t}} q_r^{(0)} \\
\Omega^{(2)}(\tilde{t})\partial_\Psi I_a^{(0)} &= q_r^{(1)}\partial_{q_r} G_a^{(1)}(q_r^{(0)}, I_c^{(0)}, \tilde{t}) + I_b^{(1)}\partial_{I_b} G_a^{(1)}(q_r^{(0)}, I_c^{(0)}, \tilde{t}) \\
&\quad +G_a^{(2)}\left(q_r^{(0)}, I_c^{(0)}, \tilde{t}\right) - \Omega^{(0)}(\tilde{t})\partial_\Psi I_a^{(2)} \\
&\quad -\Omega^{(1)}(\tilde{t})\partial_\Psi I_a^{(1)} - \partial_{\tilde{t}} I_a^{(1)}
\end{aligned}
$$

Two-Timescale Expansion for Generic Schwarzschild EMRIs

$$\begin{aligned}\Omega^{(0)}(\tilde{t})\partial_\Psi I_a^{(0)} &= 0\\ \Omega^{(0)}(\tilde{t})\partial_\Psi q_r^{(0)} &= \Omega_r(I_c^{(0)})\end{aligned}$$

geodesic

$$\begin{aligned}\Omega^{(0)}(\tilde{t}) &= \Omega_r[I_c^{(0)}(\tilde{t})].\\ q_r^{(0)}(\Psi,\tilde{t}) &= \Psi.\end{aligned}$$

$$\Omega^{(0)}(\tilde{t})\partial_\Psi I_a^{(1)} = G_a^{(1)}(q_r^{(0)}, I_c^{(0)}, \tilde{t}) - \Omega^{(1)}(\tilde{t})\partial_\Psi I_a^{(0)} - \partial_{\tilde{t}} I_a^{(0)}$$

$$\partial_{\tilde{t}} I_a^{(0)}(\tilde{t}) = \langle G_a^{(1)}\rangle(I_c^{(0)}(\tilde{t}),\tilde{t})$$

adiabatic

$$\hat{I}_a^{(1)} = \frac{\mathcal{I}\hat{G}_a^{(1)}}{\Omega^{(0)}(\tilde{t})}$$

$$I_a^{(1)} = \frac{\mathcal{I}\hat{G}_a^{(1)}}{\Omega^{(0)}(\tilde{t})} + \mathcal{C}_a^{(1)}(\tilde{t}).$$

post-adiabatic

$$\widetilde{\partial}_t \mathcal{C}_a^{(1)}(\tilde{t}) = \mathcal{C}_b^{(1)}(\tilde{t})\partial_{I_b}\langle G_a^{(1)}\rangle + \langle G_a^{(2)}\rangle + \frac{\langle \mathcal{I}\hat{G}_b^{(1)}\cdot\partial_{I_b}\hat{G}_a^{(1)}\rangle - \langle \hat{g}_r^{(1)}\hat{G}_a^{(1)}\rangle}{\Omega^{(0)}(\tilde{t})}.$$

where $\langle F\rangle$ is the average part and $\hat{F}=F-\langle F\rangle$ is the pure oscillation part.

The self-force terms are

$$
\begin{aligned}
g_r^{(1)} = f_r^{(1)} &\times \frac{M\Omega_r p_0^2(p_0-3-e_0^2)}{e_0[(p_0-6)^2-4e_0^2](1+e_0\cos\chi)^2} \times [2e_0-(6-p_0)\cos\chi] \\
&+ f_\phi^{(1)} \times \sqrt{\frac{p_0}{p_0-6-2e_0\cos\chi}} \times \frac{M^2\Omega_r p_0^2(p_0-3-e_0^2)}{2e_0[(p_0-6)^2-4e_0^2](1+e_0\cos\chi)^4} \\
&\quad \times \{\, [6(12+e_0^2)-(36+e_0^2)p_0+4p_0^2]\sin\chi + [4(9-e_0^2)-12p_0+p_0^2]e_0\sin 2\chi + (6-p_0)e_0^2\sin 3\chi \}
\end{aligned}
$$

$$
\begin{aligned}
G_p^{(1)/(2)} = f_r^{(1)/(2)} &\times \sqrt{\frac{p_0-6-2e_0\cos\chi}{(p_0-2)^2-4e_0^2}} \times \frac{2p_0(p_0-3-e_0^2)}{(p_0-6)^2-4e_0^2} \times [(2-p_0)e_0\sin\chi + e_0^2\sin 2\chi] \\
&- f_\phi^{(1)/(2)} \times \sqrt{\frac{p_0}{(p_0-2)^2-4e_0^2}} \times \frac{Mp_0(p_0-3-e_0^2)}{[(p_0-6)^2-4e_0^2](1+e_0\cos\chi)^2} \\
&\quad \times \{\, [3(24+8e_0^2+e_0^4)-12(6+e_0^2)p_0+(22+e_0^2)p_0^2-2p_0^3] + [24(4+e_0^2)-2(28+3e_0^2)p_0+8p_0^2]e_0\cos\chi \\
&\quad\quad + [4(6+e_0^2)-12p_0+p_0^2]e_0^2\cos 2\chi + 2(4-p_0)e_0^3\cos 3\chi + e_0^4\cos 4\chi \}
\end{aligned}
$$

The self-force terms are

$$
\begin{aligned}
G_e^{(1)/(2)} = f_r^{(1)/(2)} \times \sqrt{\frac{p_0 - 6 - 2e_0\cos\chi}{(p_0-2)^2 - 4e_0^2}} \times \frac{(p_0 - 3 - e_0^2)}{e_0[(p_0-6)^2 - 4e_0^2]} \\
\times \{\, (2+p_0)e_0 + [4(3-e_0^2) - 8p_0 + p_0^2]\cos\chi + (6-p_0)e_0\cos 2\chi\} \\
- f_\phi^{(1)/(2)} \times \sqrt{\frac{p_0}{(p_0-2)^2 - 4e_0^2}} \times \frac{M}{2e_0[(p_0-6)^2 - 4e_0^2](1+e_0\cos\chi)^2} \\
\times \{\, [4(108 + 72e_0^2 + 9e_0^4 - e_0^6) - 4(144 + 63e_0^2 + 4e_0^4)p_0 + 2(138 + 35e_0^2 + e_0^4)p_0^2 - 2(28 + 3e_0^2)p_0^3 + 4p_0^4]\sin\chi \\
+ [4(108 + 39e_0^2 + e_0^4) - 2(216 + 47e_0^2 - e_0^4)p_0 + 2(75 + 8e_0^2)p_0^2 - (21 + e_0^2)p_0^3 + p_0^4]e_0\sin 2\chi \\
+ [4(36 + 9e_0^2 - e_0^4) - 4(27 + 4e_0^2)p_0 + 2(13 + e_0^2)p_0^2 - 2p_0^3]e_0^2\sin 3\chi \\
+ [6(3 + e_0^2) - (9 + e_0^2)p_0 + p_0^2]e_0^3\sin 4\chi\}
\end{aligned}
$$

The Numerical Calculations of EoM

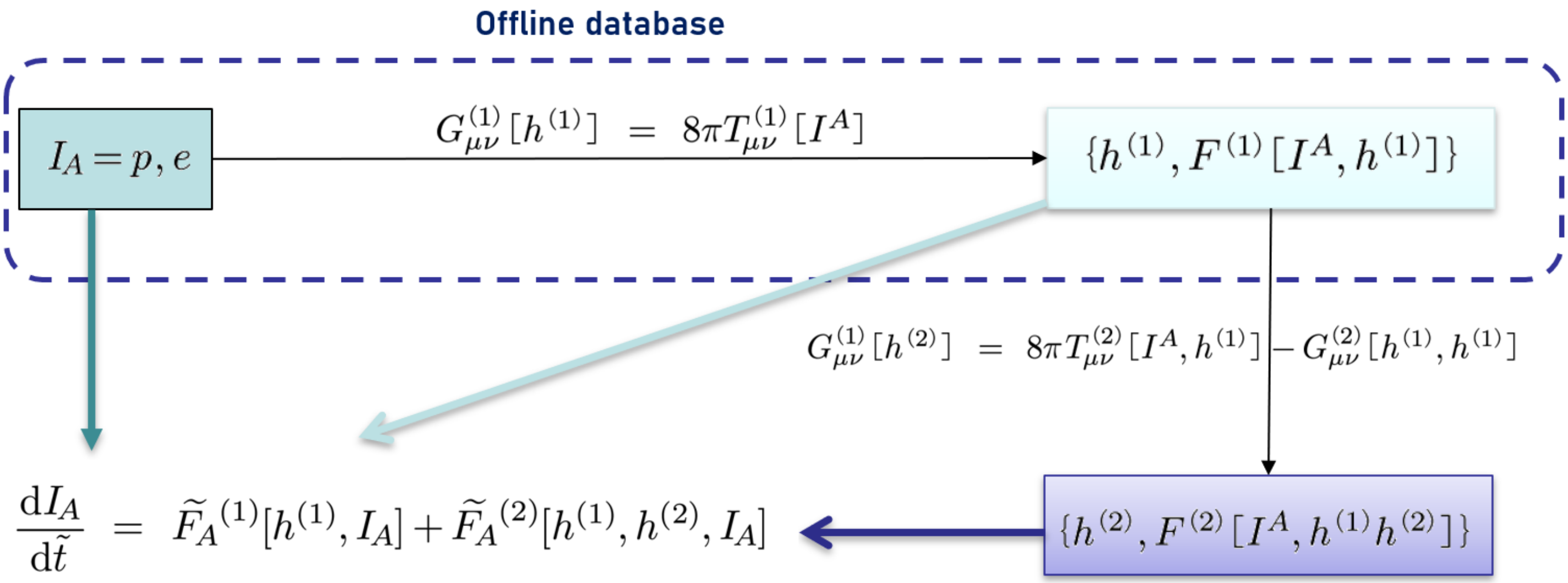

Numerical Test

We use a post-Newtonian SF formula instead of a offline SF database for simple.[6]

We compared the numerical results

- Only use osculating geodesic method (OG);
- Two-timescale expansion for adiabatic order (0PA);
- Two-timescale expansion for 1st-post-adiabatic order (1PA);(including 2SF term)

6. Wei YX, Zhu XL, Zhang JD,et al. PRD, 2025, 112(6): 064048.

Numerical Test

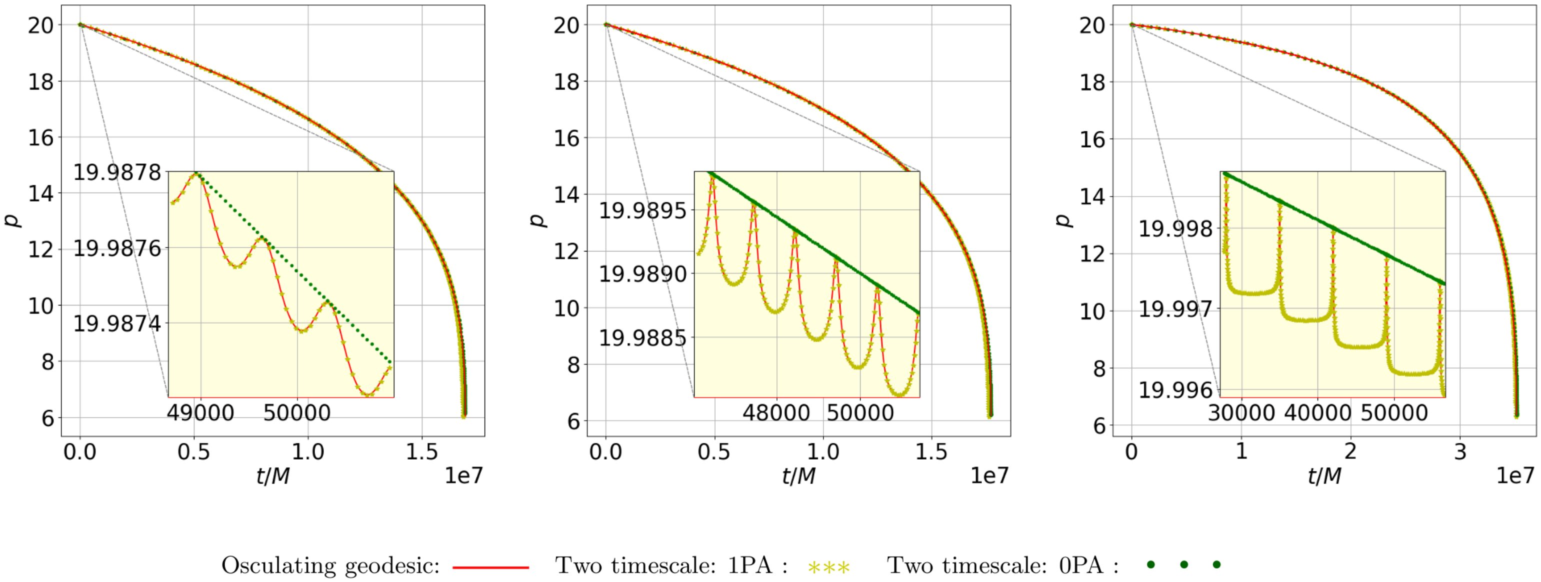

The 1PA evolution of (p,e) are close to OG results whlie 0PA results only give a average behaviour.$\varepsilon=10^{-4}$,$e=0.1/0.5/0.9$ for three columns.

Numerical Test

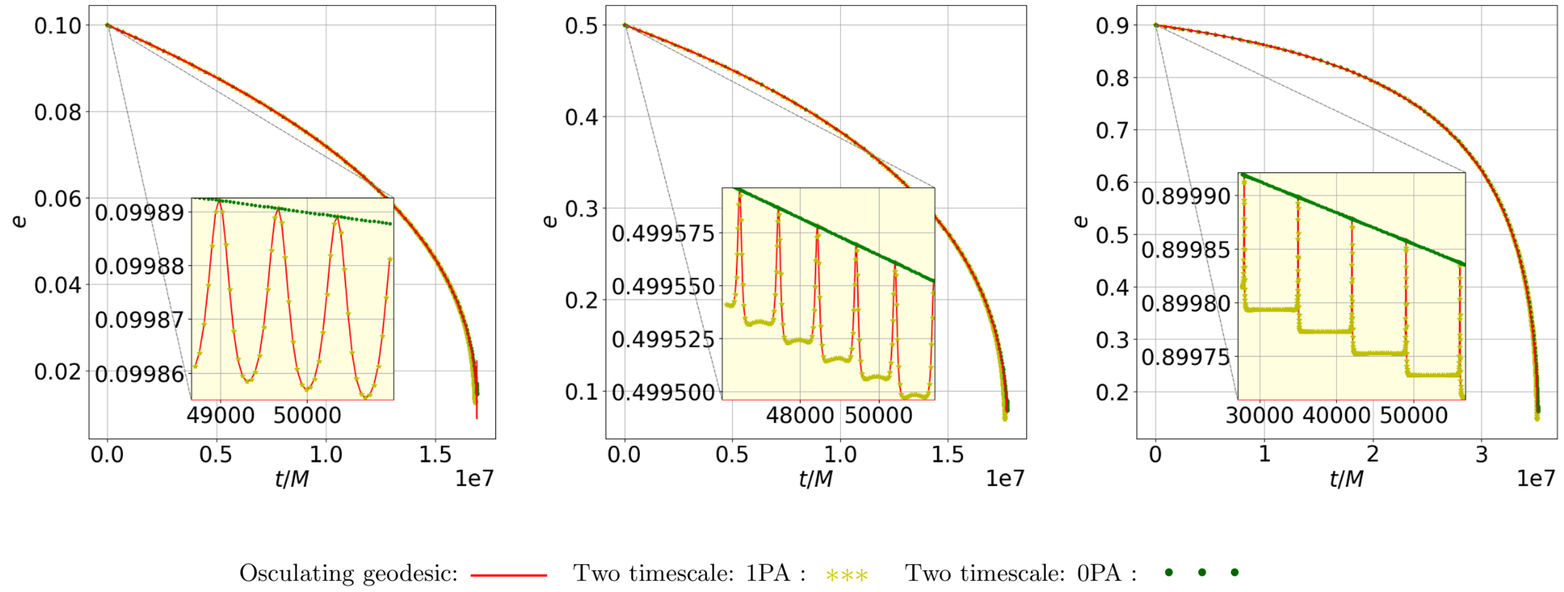

The 1PA evolution of (p,e) are close to OG results whlie 0PA results only give a average behaviour.$\varepsilon=10^{-4}$,$e=0.1/0.5/0.9$ for three columns.

Numerical Test

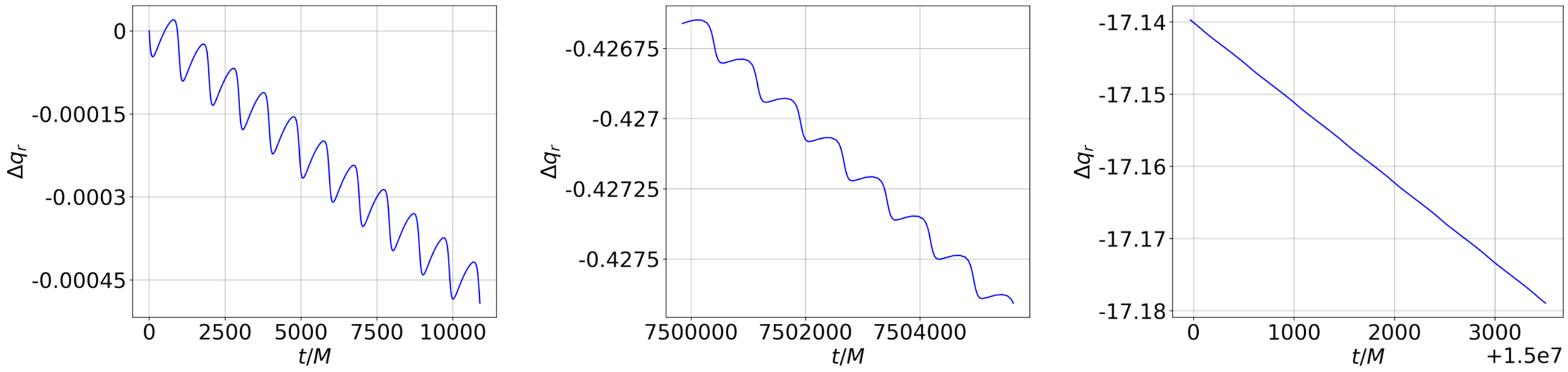

$$\varepsilon = 10^{-5}, e = 0.5$$

The error of Δq_r and Δq_ϕ grow linearly to ε, until the system near the plunge phase, where the basic assumptions of two-timescale expansion breakdown.

Numerical Test

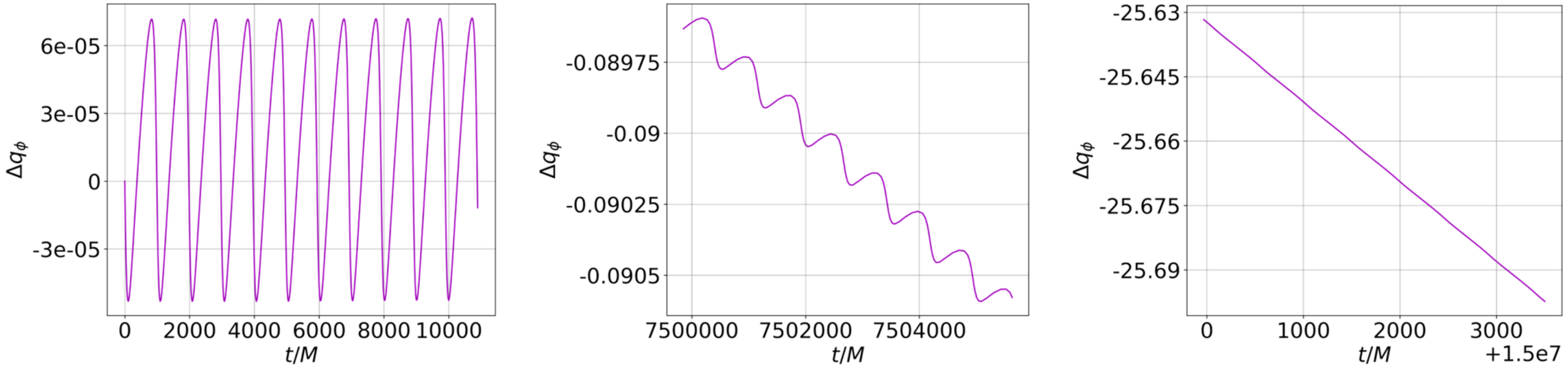

$$\varepsilon=10^{-5}, e=0.5$$

The error of Δq_r and Δq_ϕ grow linearly to ε, until the system near the plunge phase, where the basic assumptions of two-timescale expansion breakdown.

Numerical Test

e	ε	OG	0PA	1PA
0.1	10^{-3}	4min	10s	30s
	10^{-4}	25min		
	10^{-5}	168min		
0.5	10^{-3}	4min	20s	50s
	10^{-4}	25min		
	10^{-5}	139min		
0.9	10^{-3}	3min	30s	90s
	10^{-4}	25min		
	10^{-5}	133min		

$$p = 20M$$

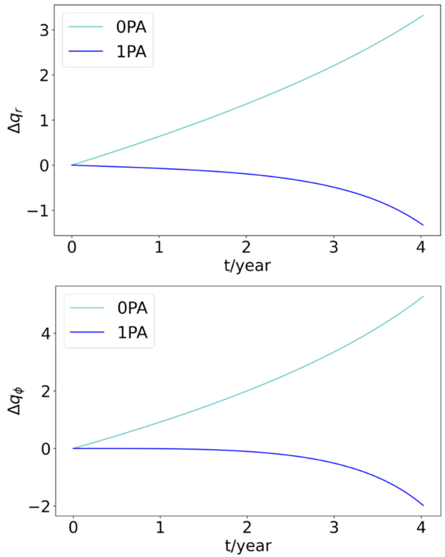

$$(M, \varepsilon, p, e) = (10^6 M_\odot, 10^{-5}, 15, 0.3)$$

The 1PA calculation time is irrelevant to ε. The 1PA phase error <0.1 rads for first 2 years.

Overview

Conclusion

In this work, for generic orbit Schwarzschild EMRIs,we have:

- Given the analytic formula of puncture fields to the sub-leading order;
- Given the analytic formula of two-timescale expansion of EoM to the 1PA order.
- Verify the accuracy and efficiency of our method by numerical tests.

  We show that the 1PA methods significantly speed up the calculation from hours to seconds where remain a high accuracy for phase error <0.1 rad for about 2 years.

Future Plan:

- Prepare the 2nd SF database. Due to the high computational cost for numerical calculate the puncture fields, some simplification methods[7] must be introduced to optimize the efficiency.

7. Zhang C, Cai R, Fu G, et al. arXiv preprint arXiv:2505.19732, 2025.

Thanks for Watching!!